High Frequency Matched Field Processing

W.S. Hodgkiss, W.A. Kuperman, J.J. Murray, G.L. D'Spain, and L.P. Berger

Marine Physical Laboratory
Scripps Institution of Oceanography
La Jolla, CA 92093-0701

Abstract

Results are discussed from a high frequency (0.9-5.7 kHz), very shallow water (<10 m) experiment exploring the feasibility of carrying out matched field processing in this frequency and water depth regime. The data was received on a 22-element vertical array with interelement spacing one half-wavelength at 4 kHz. An acoustic source broadcasting a multitone comb was towed along radial tracks with maximum range from the array of several hundred meters. One incoming track was selected for analysis using conventional (nonadaptive) matched field processing. The structure of the range-depth ambiguity surface (incoherently averaged across frequency) is shown as well as the time-evolving range surface (for a fixed source depth). In addition, time series of the range and depth maxima are shown along with their corresponding correlation values. Although a very simple range-independent environmental model was used to generate the matched field replica vectors, the results clearly demonstrate the ability to track the motion of the source and resolve its position to on the order of 0.5 m in depth and 10 m in range.

1. Introduction

As a generalization of conventional (plane wave) beamforming, matched field processing (MFP) measures the similarity between the data observed on an array of sensors and the complex wave field predicted by a full-wave propagation model for a source at a given range, depth, and azimuth [1-2]. MFP has received a great deal of attention recently and impressive broadband detection, localization, and tracking results have been obtained in shallow water (< 200 m) at low-to-mid frequencies (< 600 Hz) [3-4].

Here we discuss the results from a high frequency (0.9-5.7 kHz), very shallow water (<10 m) experiment exploring the feasibility of carrying out matched field processing in this frequency regime. Section 2 will describe the experiment, array geometry, and the bathymetry observed along the source tow track. The results from performing conventional (nonadaptive) matched field processing on the data then are presented in Section 3. Lastly, a summary is provided in Section 4.

2. Experiment Description

The experiment was conducted on 15 October 1996 in San Diego Bay in the vicinity of the Scripps Marine Facilities pier. A chart of the area prepared a few months prior to the experiment indicates that the bathymetry generally is flat in the area north of the pier where two of the three source tow events were conducted.

Figure 1 shows the experiment geometry and a sound speed profile derived from CTD data collected immediately after the source tow event analyzed in Section 3. The vertical array consisted of 22 elements positioned as shown in the upper part of the water column. The array was deployed from the pier with a heavy weight on the bottom keeping it straight. The uppermost array element was 0.67 m below the surface and the interelement spacing was 0.188 m (approximately one half-wavelength at 4 kHz). The time series from each array element was sampled at 48 kHz.

Source tows were carried out with a small boat equiped with differential GPS for accurate positioning. Bathymetry was measured during the source tows with a high frequency echo sounder. Figure 1 also shows the bathymetry measured over the north-to-south source tow track for the data discussed in Section 3. Over the range interval 150-175 m, the track cuts across a small trench with ridges on both sides. This broad east-west feature is evident on the chart of the area north of the pier.

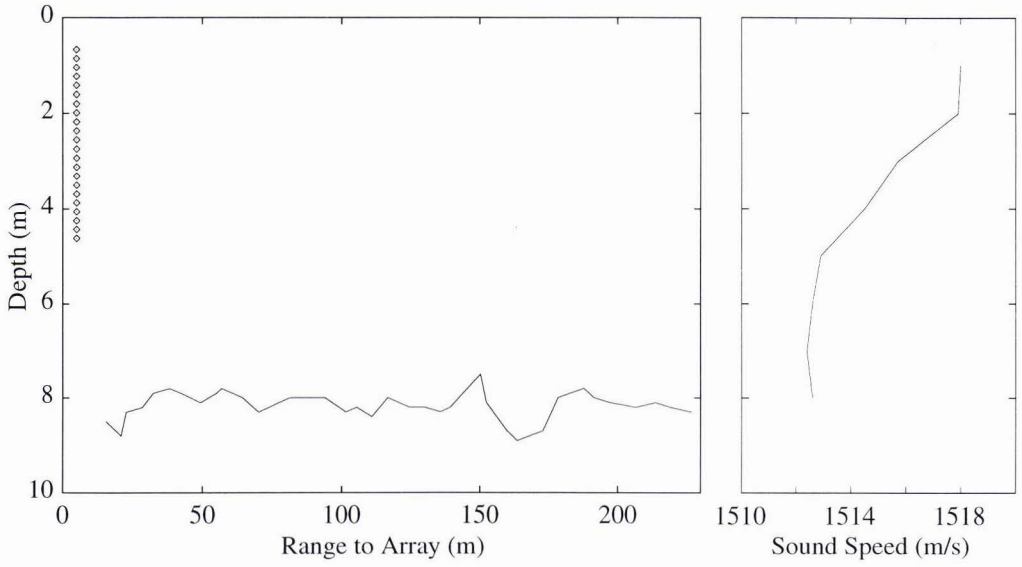

Figure 1. Experiment geometry and sound speed profile. The 22 element vertical array was located in the upper part of the water column. A small trench with slight ridges on both sides was present in the range interval 150-175 m.

During the source tow events, a J-11 was deployed to a depth of approximately 3.8 m and transmitted CW tonals at 0.9, 1.3, 2.4, 3.5, 4.6, and 5.7 kHz.

3. Data Analysis

We selected for analysis the last 3.0 minutes of data from a north-to-south source tow track. The bathymetry for this track is shown in Figure 1. The range of the source to the array was approximately 225 m at the beginning of the track and approximately 15 m at the end of the track.

For simplicity, a range independent environmental model was used to compute replica vectors. The sound speed profile is shown in Figure 1. Due to lack of detailed geoacoustic information on the bottom, representative parameters for a sand-silt-clay half-space were used [5] (compressional sound speed: 1550 m/s, compressional attenuation: 0.35 db/m/kHz, and density: 1.5 g/cm^3). Matched field replica vectors were calculated using the Kraken normal mode code [6]. Since only two modes were predicted to be excited at 0.9 kHz and three modes at 1.3 kHz, these lowest two frequencies of the source tow data were not included in the processed results.

Preprocessing of the array data consisted of computing 50% overlapped, 8192-point (Kaiser-Bessel windowed) FFT's of the hydrophone time series and extracting the (5.86 Hz wide) bins containing the source tow frequencies. At each frequency f_i, a data vector was formed at time t_j from the appropriate complex bin value from each element of the array $\mathbf{X}(f_i,t_j)$. Estimates of the array element covariance matrix were generated by averaging the outer products of successive data vectors:

$$\mathbf{K}(f_i,t) = \frac{1}{N_t} \sum_{j=1}^{N_t} \mathbf{X}(f_i,t_j)\mathbf{X}^H(f_i,t_j) \tag{1}$$

where $N_t = 5$ (0.43 s of data) and H indicates complex conjugate transpose.

Narrow-band, conventional matched field processing was implemented by computing the normalized quadratic form:

$$C(f_i,r,d,t) = \frac{g^H(f_i,r,d)\mathbf{K}(f_i,t)g(f_i,r,d)}{Tr(\mathbf{K}(fi,t))\ |g(f_i,r,d)|^2} \tag{2}$$

where $g(f_i,r,d)$ is the complex wave field (replica vector) predicted by the full-wave propagation model for a source at range r and depth d away from the array and $Tr(\mathbf{K}(f_i,t))$ is the trace of the covariance matrix $\mathbf{K}(f_i,t)$.

Then, the individual frequency matched field processing results were averaged incoherently across frequency:

$$C(r,d,t) = \frac{1}{N_f} \sum_{i=1}^{N_f} C(f_i,r,d,t) \tag{3}$$

As an example of (3), the range-depth ambiguity surface at t = 1.7 min is shown in Figure 2. Although ambiguous sidelobes are present, the source is localized easily at r = 90 m and d = 3.8 m with resolution on the order of 10 m in range and 0.5 m in depth.

In the processing, successive ambiguity surfaces as in Figure 2 are computed. Since the source depth was known to be approximately constant during the source tow, one useful way to visualize the time-evolving structure of the matched field processor output is to display a slice of each ambiguity surface at a given depth. Figure 3 shows the time-evolving range surface for d = 3.8 m. The incoming track of the source clearly is visible.

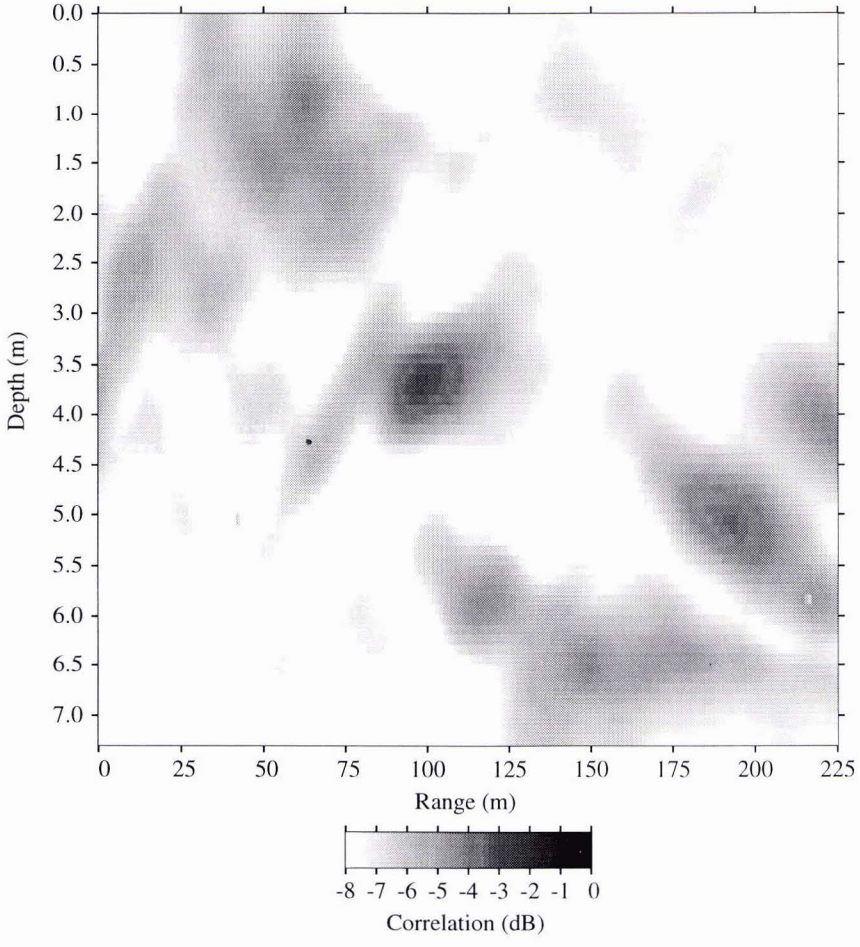

Figure 2. Range-depth ambiguity surface at t = 1.7 min averaged across the source tow tonals at 2.4, 3.5, 4.6, and 5.7 kHz. The source is localized at r = 90 m and d = 3.8 m.

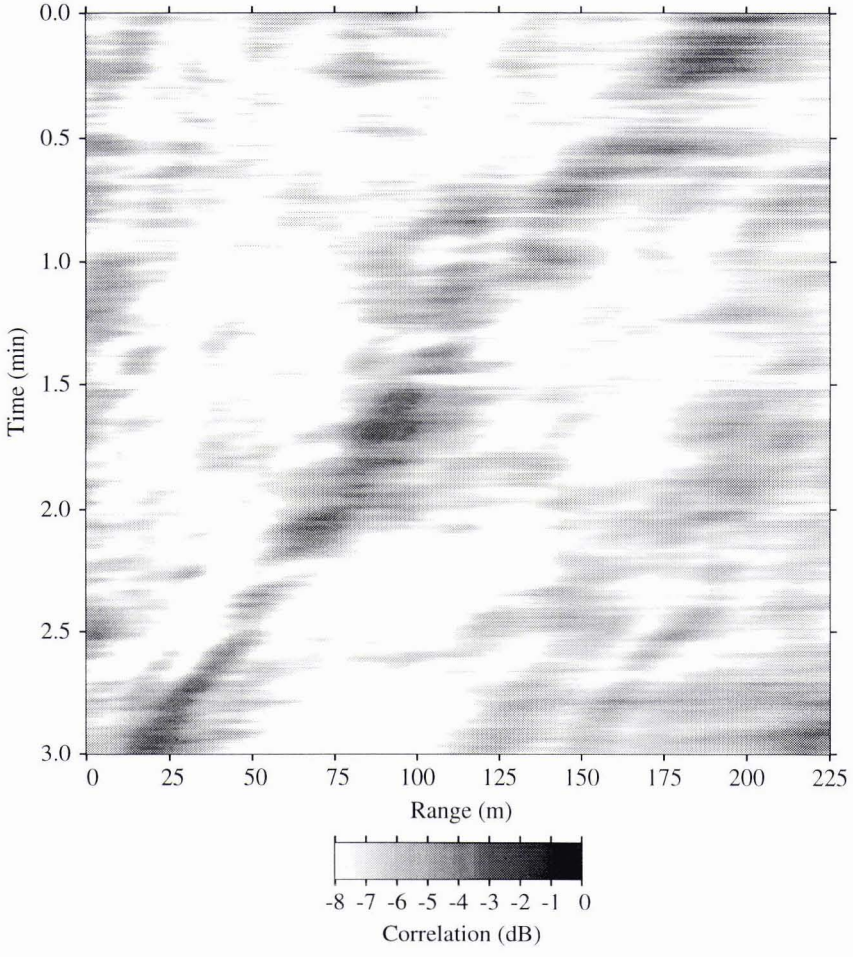

Figure 3. Time-evolving range range surface for d = 3.8 m averaged across the source tow tonals at 2.4, 3.5, 4.6, and 5.7 kHz. The source is closing on the array as time increases.

The time series of range-depth maxima of the successive ambiguity surfaces provides additional information on how well the matched field processor is able to track the source. Figure 4 displays the peak ranges as the source closes on the array along with the true range (based on DGPS measurements of source and array position). Similarly, Figure 5 displays the peak depths along with the bathymetry under the souce as measured by the echo sounder. Although the source track can be discerned in both figures, a substantial number of ambiguous peaks are seen when the source is in the vicinity of the trench (0.4-1.2 min). This is not surprising considering the simple, range-independent environmental model used for computing the matched field replica vectors.

Lastly, the time series of correlation values for the range-depth maxima of the successive ambiguity surfaces is shown in Figure 6. During the last half of the track where the range-independent environmental model is reasonably accurate, the correlation values generally are between -3 and -4 dB. At the high signal-to-noise ratios present in these data, a perfect match between the observed data and predicted replica field would yield a correlation value of 0 dB.

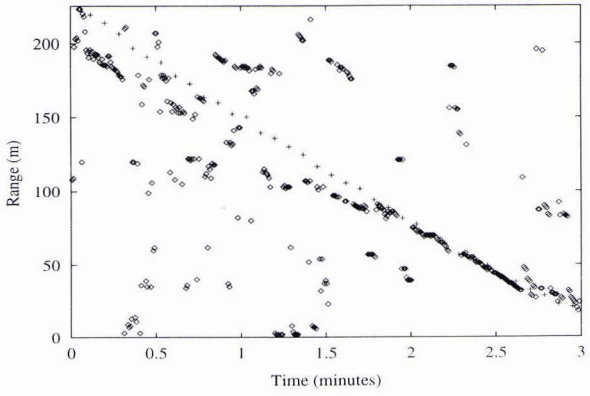

Figure 4. Time series of peak ranges from the individual range-depth ambiguity surfaces. The true source-array range is indicated by +'s.

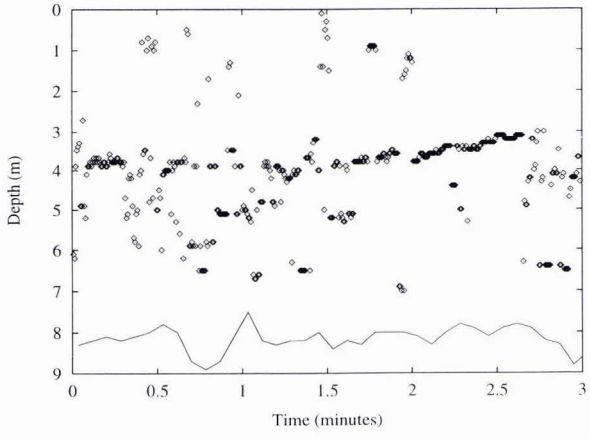

Figure 5. Time series of peak depths from the individual range-depth ambiguity surfaces. The bathymetry under the source also is displayed.

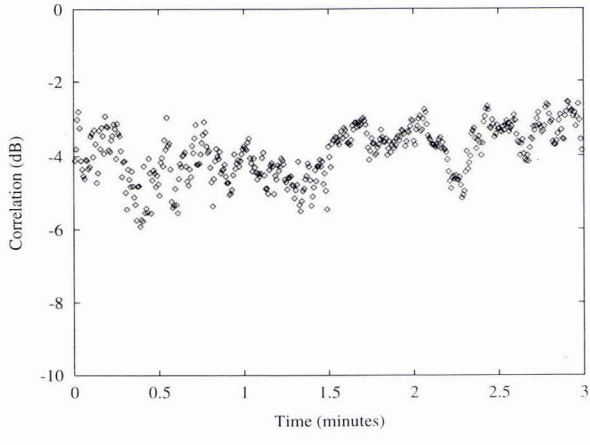

Figure 6. Time series of correlation values for the range-depth maxima from the individual range-depth ambiguity surfaces.

4. Summary

The focus of this paper has been on exploring the feasibility of carrying out broadband matched field processing on high frequency (0.9-5.7 kHz) source tow data in very shallow water (<10 m). A 4.0 m aperture, 22-element vertical array received multitone transmissions from a source towed at approximately 3.8 m depth and ranges of up to several hundred meters. Conventional (nonadaptive) matched field processing was performed on the data from an incoming track where the source range decreased from 225 m to 15 m over 3.0 min. The structure of the range-depth ambiguity surface (incoherently averaged across frequency) was shown as well as the time-evolving range surface (for a fixed source depth of 3.8 m). Time series of the range and depth maxima also were shown along with their corresponding correlation values. Although a very simple range-independent environmental model was used to generate the matched field replica vectors, the results clearly demonstrate the ability to track the motion of the source and resolve its position to on the order of 0.5 m in depth and 10 m in range.

Acknowledgements

This work was sponsored by the Office of Naval Research, Code 321OA.

References

[1] A.B. Baggeroer, W.A. Kuperman, and P.N. Mikhalevsky, "An overview of matched field methods in ocean acoustics," *IEEE J. Oceanic Engr.* vol. 18(4), pp. 401-424 , 1993.

[2] F.B. Jensen, W.A. Kuperman, M.B. Porter, and H. Schmidt. *Computational Ocean Acoustics*. NY: American Institute of Physics , 1994.

[3] N.O. Booth et. al., "Source localization with broadband matched field processing in shallow water," *IEEE J. Oceanic Engr.* vol. 21(4), pp. 402-412, 1996.

[4] Z. Michalopoulou and M.B. Porter, "Matched-field processing for broad-band source localization," *IEEE J. Oceanic Engr.* vol. 21(4), pp. 384-392, 1996.

[5] E.L. Hamilton, "Geoacoustic modeling of the sea floor," *J. Acoust. Soc. Am.* vol. 68(5), pp. 1313-1340, 1980.

[6] M.A. Porter, "The KRAKEN normal mode program," SACLANTCEN SM-254, SACLANT Undersea Research Centre, La Spezia, Italy, 1991.